Kinetics of back reaction between radiolytic products initiated by radiation-induced voids in NaCl

Kinetics of back reaction between radiolytic products initiated by radiation-induced voids in NaCl

A A Turkin[1], V I Dubinko[1], D I Vainshtein[2] and H W den Hartog[2]

[1] National Science Centre Kharkov Institute of Physics and Technology, 61108 Kharkov, Ukraine
[2] Solid State Physics Laboratory, University of Groningen, 4 Nijenborgh,
NL-9747 AG Groningen, The Netherlands

E-mail: anatole.turkin@kipt.kharkov.ua, dubinko@kipt.kharkov.ua, d.vainshtein@phys.rug.nl
and h.w.den.hartog@phys.rug.nl

Abstract

A time-dependent model is formulated for the chemical reaction between
sodium colloids and gas bubbles, which are brought into contact with each
other by the growing voids. It is shown that in this exothermic reaction, heat
is released much faster than it is dissipated by conduction to the surrounding
salt. This results in a large and sudden temperature and pressure increase in
the void, which is analysed in detail. The effect on the mechanical stability of
NaCl under irradiation is discussed.

1. Introduction

The behaviour of rock salt under irradiation has been the subject of numerous studies because
it is one of the candidate host rock materials for radioactive waste storage and its fundamental
properties can be used to understand the radiation stability of many other ionic systems,
including ceramics [1–11]. Exposure of NaCl samples to ionizing radiation is known to result
in the production of chlorine 'bubbles' (or rather solid or liquid chlorine precipitates, since
the pressure inside them is too high for the liquid–gas transition) formed by agglomeration
of H centres and of the complementary inclusions of metallic sodium ('colloids') formed
by agglomeration of F centres [1, 2]. The volume fraction of chlorine bubbles and sodium
colloids is a measure for the stored energy. The higher it grows, the more potentially unstable
the material becomes. But the actual mechanical stability of the sample depends strongly on
a scenario of stored energy release. Our experiments [3–6] on heavily irradiated pure, doped
and natural rock-salt samples, which had been exposed to 0.5 MeV electrons up to fluences
of 6×10^{18} electrons cm^{-2} (i.e. about 300 Grad or 130 dpa (displacements per anion)), show
that with increasing irradiation dose, voids are formed followed by their transition to large
(hundreds of nm in size) penny-shaped cracks (figure 1) resulting in a subsequent explosion-
driven fracture of the material (figure 2(a)). In general, the amount of radiation-induced stored
energy (SE) increases linearly with the intensity of the endothermic latent heat peaks of melting
(LHM) of Na, which is proportional to the volume fraction of chlorine bubbles and sodium
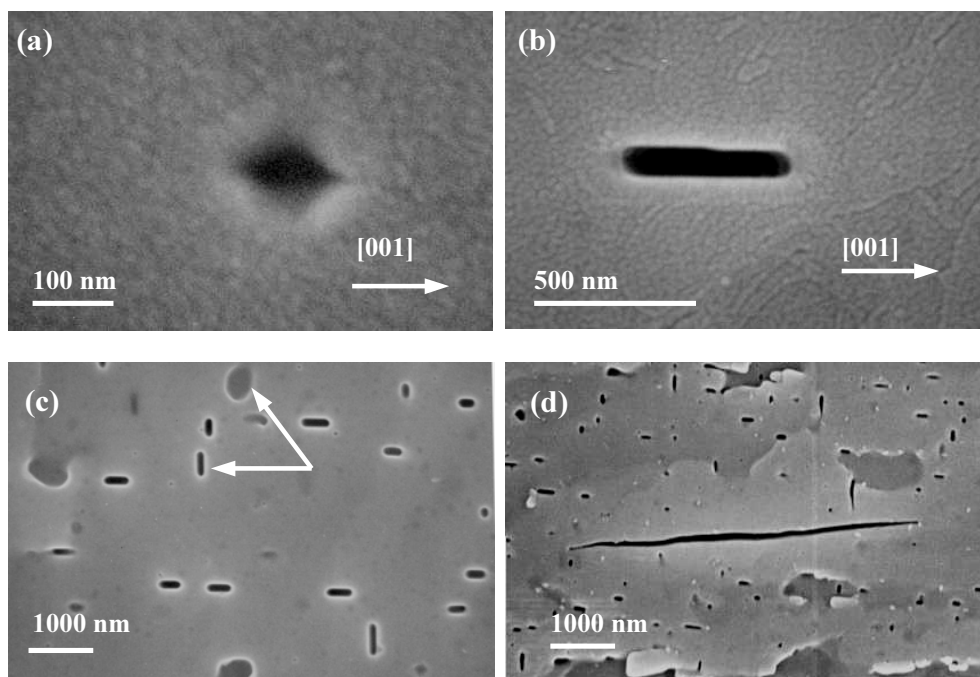
Figure 1. SEM micrographs showing vacancy voids and cracks in natural rock-salt crystals irradiated with 0.5 MeV electrons at 100 °C. (a) An equiaxial void at high resolution after irradiation to 60 Grad; the latent heat of melting (LHM) of metallic Na is 0.45 J g^{-1}. (b) The 'penny-shaped' crack formed after irradiation to 300 Grad; the LHM of metallic Na is 0.8 J g^{-1}. (c) Voids and 'penny-shaped' cracks in natural rock salt irradiated up to 300 Grad; the LHM of metallic Na is 1.2 J g^{-1}. The arrows show two cracks with different orientations. (d) The long crack formed after irradiation to 300 Grad; the LHM of metallic Na is 2.5 J g^{-1}.
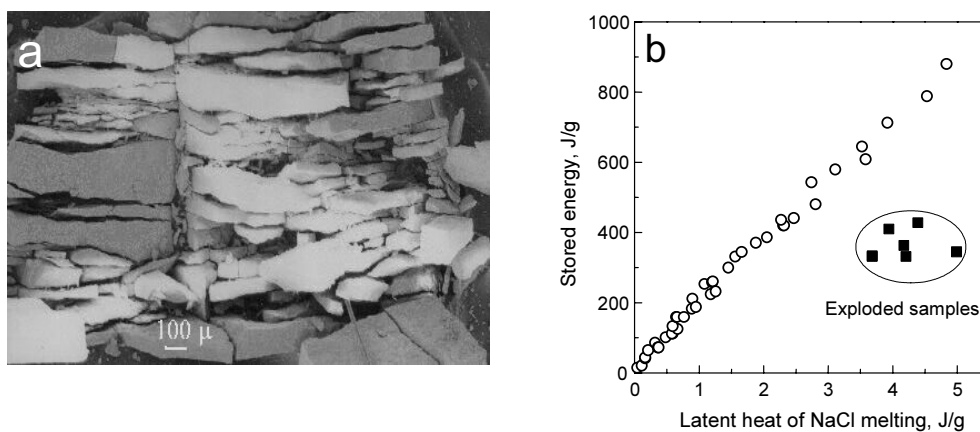

Figure 2. (a) Explosive fracture of NaCl + K (0.1 mol%) samples irradiated with 0.5 MeV electrons to 300 Grad. The SEM micrograph of the exploded sample reveals large fragments and dust-like particles. (b) Combined LHM and SE results for irradiated NaCl. For the exploded samples the SE is 30–50% lower than for unexploded ones.

colloids. However, for exploded samples the stored energy was 30–50% lower than the value expected on the basis of LHM results (figure 2(b)), which means that a considerable fraction of the radiolytic Na and Cl was involved in a back reaction and the corresponding SE has been released in the explosion process, which took place after measuring the latent heat effects, but prior to the measurement of the SE [6]. Mechanical cleavage of the irradiated samples containing voids did not result in explosive fracture, but we have recorded the explosions with fast video techniques in conjunction with optical microscopy during post-irradiation heating in the temperature range between 100 °C and 250 °C. Samples with large voids exploded at lower temperatures than samples with smaller voids. In this case it was possible to carefully control the amount of stored energy by measuring the latent heat of melting of Na before and after the explosion. The LHM decrease during the explosion confirmed that the latter was indeed due to the release of radiation-induced SE [6].

We have proposed a new model [7–9], in which voids are shown to arise from chlorine bubbles either due to a fluctuative transition through the critical point [7, 8] or due to collisions between chlorine bubbles and sodium colloids, which may result in the explosive formation of overcritical voids [9]. Once formed, the voids can grow quickly (as compared to the colloid growth [8]) via the agglomeration of electroneutral vacancy pairs at their surfaces with the result that the void sizes exceed the mean distance, first, between bubbles and, then, between colloids. During their growth, the voids absorb fine chlorine bubbles and they accumulate large numbers of chlorine molecules before the collision between voids and colloids starts, which ignites a powerful back reaction resulting in a drastic and very rapid temperature and pressure increase within a chlorine-filled void [10]. In the present paper we will consider the thermodynamic and kinetic aspects of the back reaction inside the voids focusing on the reaction-induced evolution of temperature and pressure within voids as a function of the time.

2. Microstructural evolution prior to the back reaction

According to the present model [9] (figure 3), chlorine bubbles (a few nm in size) are the most finely dispersed extended defects (ED) in the system: $R_B < R_C < R_V$ (here the subscripts refer to bubbles, colloids and voids, respectively), i.e. a growing void collects chlorine gas by sweeping the bubbles with its moving boundary. The chlorine molecules within the 'bubbles' are in a solid or liquid state due to a superhigh pressure (in the GPa range), but after collision with a void they become a gas. One can estimate the number of chlorine atoms, n_{Cl}, captured by a void of radius R_V as a product of the void volume and the bubble volume fraction, V_B, divided by the chlorine atomic volume, ω_{Cl}:

$$n_{Cl} = \frac{4\pi}{3} R_V^3 \frac{V_B}{\omega_{Cl}}. \tag{1}$$

Note that n_{Cl} is determined by the amount of chlorine stored in bubbles per unit volume and so it does not depend on the absolute value of the void growth rate. The bubble volume fraction increases with irradiation dose at the same rate as the colloid volume fraction:

$$V_C = \frac{\omega}{\omega_{Cl}} V_B$$

due to the balance between sodium and chlorine atoms stored in the unit volume of the matrix, where ω is the atomic volume of NaCl. Accordingly, the gas pressure within the voids (where it is in molecular form) is also determined by the colloid volume fraction:

$$P = \frac{(n_{Cl}/2)k_B T}{(4\pi/3)R_V^3} = \frac{k_B T}{2\omega_{Cl}} V_B = \frac{k_B T}{2\omega} V_C \tag{2}$$

where we have used the equation of state of an ideal gas, which is valid in this pressure region. k_B is the Boltzmann constant. An estimate for an irradiation experiment carried out at 100 °C shows that even at very large colloid concentrations of $V_C \approx 10\%$, the pressure is 5×10^{-3} GPa (50 atm), which is still lower than the surface tension of a void as large as 200 nm. This implies that these pressures do not affect the void bias, which controls the void diffusion growth. However, the chlorine accumulation in voids provides a very important possibility for explosive back reaction with metallic sodium when growing voids start hitting colloids, which is a much more powerful reaction than that induced by direct colloid–bubble collisions. It is expected to occur when the radius of the voids approaches the mean distance between colloids. The corresponding relation between the void size and the number of colloids per unit volume is

$$R_V = \left(\frac{3}{4\pi N_C} \right)^{1/3}. \tag{3}$$

Here, N_C is the colloid number density.

The amount of released energy in the back reaction is proportional to the energy released due to the formation of one NaCl molecule, q_{NaCl}, and to the number of NaCl molecules formed as a result of the local back reaction. The latter is equal to the mean number of sodium atoms in a colloid, which is close to the number of chlorine atoms accumulated in the void at the time of the collision, and which is two orders of magnitude larger than that in one bubble. The released energy heats up the reaction products inside the void, resulting in an instantaneous temperature and pressure increase, which has been estimated in [10] as follows:

$$\Delta T = \frac{2}{3} \frac{q_{NaCl}}{k_B} \geqslant 2 \times 10^4 \text{ K} \qquad \Delta P \geqslant \frac{2}{3} \frac{q_{NaCl}}{\omega} V_C. \tag{4}$$

This estimate has been made under the assumption that there is no exchange of heat between the hot gas within the void and the surrounding crystal lattice, which has a high heat capacitance as compared to the hot gas. The actual temperature increase will therefore be smaller than the one given by (4). One should take into account realistic rates of reaction between Na and Cl within the voids, the shape of the initial voids (i.e. approximately spherical) and furthermore realistic relaxation times for the heat exchange with the surrounding lattice, which will be derived below.

3. The back reaction model

In this section we will formulate a model for calculating the temperature and pressure increase inside a void due to an exothermic reaction between radiolytic products. Initially, due to the reaction between the Na atoms and the Cl_2 molecules at the colloid surface, the local system is warmed up, and the solid colloid is transformed into vapour inside the void. After that the (rapid) back reaction proceeds in the gas phase.

The reaction between Na and Cl_2 falls into the category of fast exo-ergic reactions, which have no 'threshold energy' [12]. It has been established experimentally that the reaction between alkali and halogen atoms/molecules takes place during practically all collisions of the appropriate particles. The estimations suggest that the effective cross-sections for these collisions are considerably (up to ten times) larger than the gas-kinetic cross sections [13]. The 'harpoon mechanism', proposed by Polanyi [12], explains the very high reaction rate as follows. Schematically, the reaction proceeds in two stages:

$$\begin{aligned} &\text{Na} + \text{Cl}_2 \rightarrow \text{NaCl} + \text{Cl} \\ &\text{Na} + \text{Cl} \rightarrow \text{NaCl}. \end{aligned} \tag{5}$$
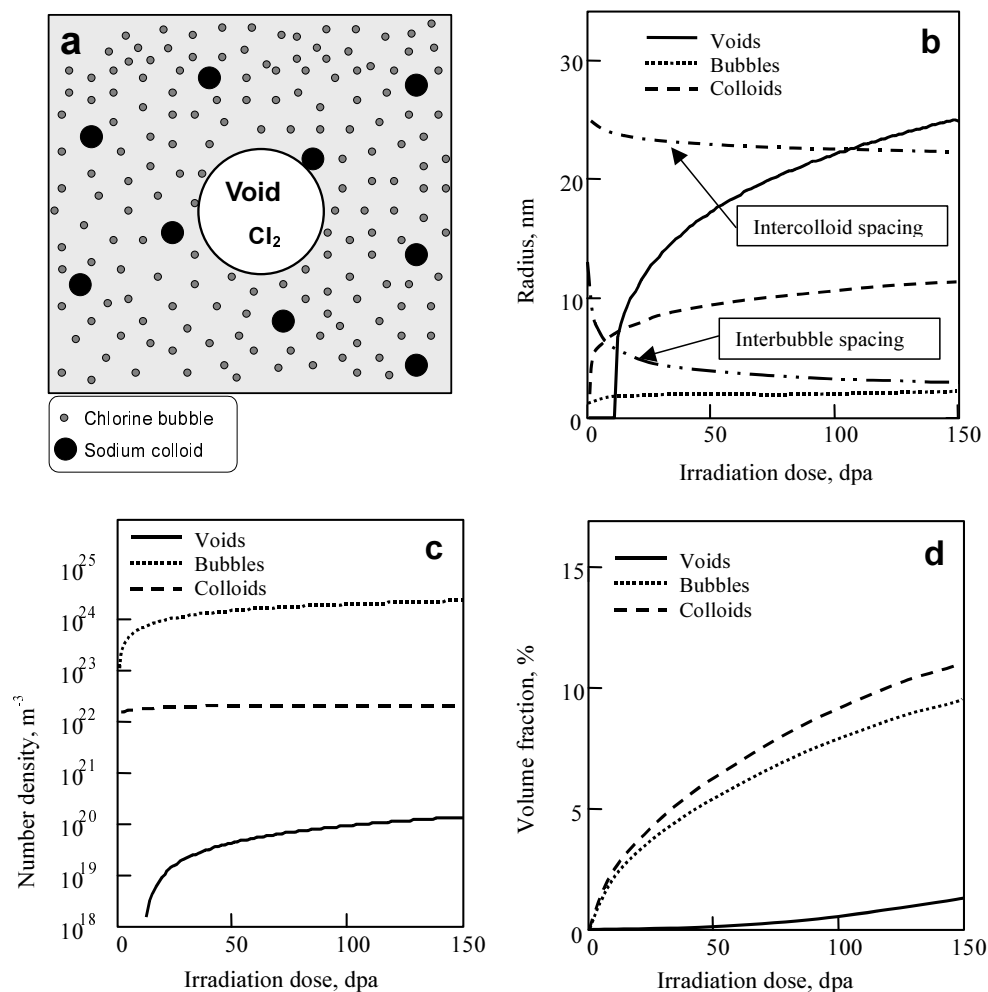
Figure 3. Evolution of bubbles, colloids and voids with increasing irradiation dose (in displacements per anion, dpa) calculated in reference [9]. (a) A schematic illustration. (b) The intersection between the colloid radius and interbubble spacing curves indicates the beginning of the explosive back reaction due to collisions between the bubbles and colloids resulting in the formation of voids, which grow to sizes exceeding the intercolloid spacing and thus provide for the following and larger step of the explosive back reaction. (c) and (d) show the corresponding number densities and volume fractions of radiolytic products.

The first stage of the reaction is envisaged as the transfer of a valence electron of the alkali metal atom to the halogen molecule. Such a transfer is possible even when reactants are quite a few ångströms apart. Once the transfer takes place and an ion pair (e.g. $Na^+Cl_2^-$) is formed, a strongly attractive Coulombic force brings the two ions together; this is followed by the formation of a stable NaCl molecule and the rejection of the Cl atom. The metal atom, in effect, uses its valence electron as a 'harpoon' in order to pull in the halogen molecule.

In this paper, we will use a phenomenological model of the diffusion-controlled bimolecular reaction. It is assumed that after the collision with a colloid, as a result of the very rapid increase of the local temperature, the void is filled with a homogeneous mixture of Na and Cl_2 gas. The concentrations of Na, Cl_2, Cl and NaCl particles in the gas change with time

according to the following reaction rate equations:

$$\frac{dc_{Na}}{dt} = -\alpha_{NaCl_2} c_{Na} c_{Cl_2} - \alpha_{NaCl} c_{Na} c_{Cl}$$

$$\frac{dc_{Cl_2}}{dt} = -\alpha_{NaCl_2} c_{Na} c_{Cl_2}$$

$$\frac{dc_{Cl}}{dt} = \alpha_{NaCl_2} c_{Na} c_{Cl_2} - \alpha_{NaCl} c_{Na} c_{Cl} \qquad (6)$$

$$\frac{dc_{NaCl}}{dt} = \alpha_{NaCl_2} c_{Na} c_{Cl_2} + \alpha_{NaCl} c_{Na} c_{Cl}.$$

Here concentrations are defined in terms of atomic fractions. The atomic fractions c can be converted into volume concentrations according to the relationship $n = c/\omega$, where the atomic volume of NaCl, ω, is approximately equal to the atomic volume of metallic Na.

According to Smoluchowski [14], the reaction rates α_{ij} are given by

$$\alpha_{ij} = \frac{4\pi r_{ij}}{\omega}(D_i + D_j) \qquad i, j = Na, Cl, Cl_2, NaCl \qquad (7a)$$

where D_i and D_j are the diffusion coefficients, and r_{ij} is the distance of a closest approach between species i and j, which is assumed to be the sum of the radii of the participating atoms/molecules. According to the kinetic theory of gases, the diffusion coefficient equals

$$D_i = \frac{1}{3}\lambda_i \langle v_i \rangle \qquad (7b)$$

where λ_i is the collision-free path of the i-type particle and

$$\langle v_i \rangle = \sqrt{\frac{8k_B T}{\pi m_i}}$$

is its average thermal velocity (m_i is the mass.) The collision-free path in the gas mixture of reactants and reaction products (NaCl molecules) is defined as (see, e.g., [15])

$$\lambda_i = \omega\left(\sum_j c_j \sigma_{ij} \sqrt{1 + \frac{m_i}{m_j}}\right)^{-1}$$

$$\sigma_{ij} = \sigma_{ji} = \pi(r_i + r_j)^2 \qquad (8)$$

where σ_{ij} is the effective gas-kinetic cross section, r_i is the atomic radius.

Our aim is to find the time dependence of temperature inside the void due to the concurrent processes of heat generation in the void and heat absorption by the surrounding NaCl matrix. The heat that is released in the reaction at a rate $q_{NaCl} dc_{NaCl}/\omega dt$ is distributed between gas particles in the void and dissipates into the NaCl matrix. The heat balance is given by

$$\frac{4\pi}{3} R_V^3 q_{NaCl} \frac{dc_{NaCl}}{\omega dt} = \frac{4\pi}{3} R_V^3 \frac{d}{\omega dt}[T(C_1(c_{Na} + c_{Cl}) + C_2(c_{NaCl} + c_{Cl_2}))] + 4\pi R_V^2 j_{out} \qquad (9)$$

where $C_1 = \frac{3}{2}k_B$ and $C_2 = \frac{5}{2}k_B$ are the specific heat capacities at a constant volume of monatomic and diatomic gases defined per particle.

In this paper we assume that no melting of the NaCl matrix occurs. To find the heat flux j_{out} we note that the heat conduction is much faster inside the void than in the matrix; therefore the temperature $T(t)$ inside the void is assumed to be uniform and equal to its value at the void boundary. Under these conditions the heat flux from the void is given by [16]

$$j_{out} = \frac{k}{\sqrt{\pi a}}\frac{d}{dt}\int_0^t \frac{T(\tau) - T_0}{\sqrt{t - \tau}} d\tau + \frac{k}{R_V}(T(t) - T_0) \qquad (10)$$

where k is the coefficient of heat conductivity, $a = k/C_m d_m$ is the coefficient of temperature conductivity, C_m is the specific heat capacity of the NaCl matrix and d_m is the matrix density; T_0 is the initial (matrix) temperature.

From (6), (9) and (10) we find the equation describing the time dependence of the temperature inside the void:

$$\frac{dT}{dt} = \frac{q_{NaCl}\, dc_{NaCl}/dt + (2C_1 - C_2)T\alpha_{NaCl}c_{Na}c_{Cl}}{C_1(c_{Na} + c_{Cl}) + C_2(c_{NaCl} + c_{Cl_2})} - \frac{3\omega}{R_V}\frac{1}{C_1(c_{Na} + c_{Cl}) + C_2(c_{NaCl} + c_{Cl_2})}$$
$$\times \left[\frac{k}{\sqrt{\pi a}} \int_0^t \frac{1}{\sqrt{t - \tau}} \frac{dT(\tau)}{d\tau}\, d\tau + \frac{k}{R_V}(T - T_0) \right]. \tag{11}$$

This equation is the Volterra integral equation of the second kind with the integrable singularity in the kernel. Equations (6), (9), (11) form a complete set of integro-differential equations. The initial conditions are given by

$$T(0) = T_0 \qquad c_{Na}(0) = V_C \qquad c_{Cl_2}(0) = V_C/2 \qquad c_{Cl}(0) = c_{NaCl}(0) = 0. \tag{12}$$

Once the solution is found, the pressure inside the void can be related to the temperature as

$$P = \frac{k_B T}{\omega} \sum_i c_i \tag{13}$$

and compared with the threshold pressure required for cleavage of the matrix [18] along one of the (100) planes:

$$P_f = 0.5\sigma_f = 0.5\sqrt{\frac{EG_C}{\pi(1 - \nu^2)2R_V}} \tag{14}$$

where σ_f is the stress corresponding to the Griffith crack of length $2R_V$, E is the Young's modulus of NaCl; $G_C = 2\gamma_V$ is the total work of fracture (γ_V is the surface energy of NaCl).

4. Results of calculations

The set of equations (6), (9), (11) was solved numerically using material parameters listed in table 1. The algorithm of the solution of the problem is based on a fifth-order Cash–Karp Runge–Kutta method with monitoring of local truncation errors to ensure the accuracy and adjust the time step size [17]. The algorithm for the Volterra equation starts from the initial point and builds up the solution using the Runge–Kutta driver with an adaptive step size control. The quadrature scheme for the Volterra equation is based on a modified trapezoidal rule: the time derivative of temperature $dT(\tau)/d\tau$ in the integrand of (11) is linearly interpolated between the points at which the solution has been already found. The whole algorithm was found to be fast and efficient despite the very different timescales on which the dependent variables are changing.

Below, typical results of calculations are presented. Figure 4(a) shows the time dependences of concentrations of reagents and reaction products. According to the figure, the reaction time is of the order of several picoseconds, i.e. the reaction time involved is extremely short as compared to the time of heat losses to the surrounding matrix (figure 4(b)). The maximum temperature, T_{max}, for adiabatic conditions can be found from (9):

$$T_{max} = \frac{q_{NaCl}}{C_2} + \left(\frac{C_1}{C_2} + 0.5 \right)T_0 \tag{15}$$

where the first term coincides with the previous estimate (4), and the second one takes into account an ambient temperature, T_0.

Table 1. Material parameters used in calculations.

|	
Matrix temperature, T_0, K	400
Density of NaCl, d_m, kg m^{-3}	2165
Mass of Na atom, m_{Na}, kg	3.8×10^{26}
Mass of Cl atom, m_{Cl}, kg	5.9×10^{26}
Cl atomic radius, r_{Cl}, m	9.9×10^{-13}
Na atomic radius, r_{Na}, m	18.6×10^{-13}
Atomic volume of NaCl, m^3	4.5×10^{-29}
Young's modulus of NaCl, E, GPa	39.98
Poisson ratio, ν	0.333
Thermal conductivity of NaCl, k, W m^{-1} K^{-1}	1.15
Specific heat capacity of NaCl, C_m, J kg^{-1} K^{-1}	854
Coefficient of temperature conductivity, a, m^2 s^{-1}	6.22×10^{-7}
Heat of formation of NaCl molecule, q_{NaCl}, eV	4.253
Sound velocity in NaCl, V_{sound}, km s^{-1}	4.78
Surface energy of NaCl, γ_V, J m^{-2}	0.46
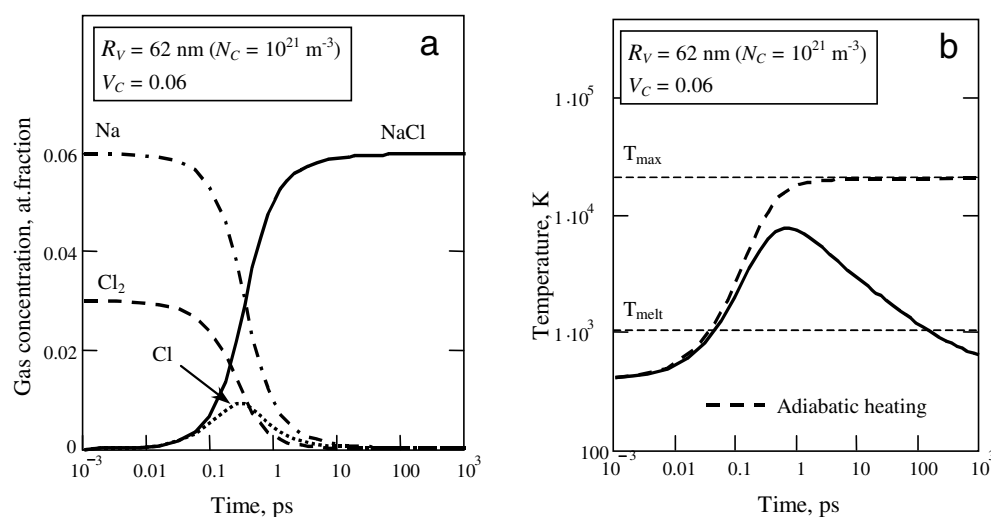
Figure 4. The time dependence of the gas concentrations (a) and temperature increase (b) within the void. The dashed line in (b) corresponds to adiabatic conditions ($j_{out} = 0$ or $R_V \rightarrow \infty$). T_{melt} is the melting temperature of NaCl. Note the logarithmic timescale.

Figure 5 shows the behaviour of the pressure inside the void as a function of the time elapsed after the beginning of the reaction for different void radii and colloid volume fractions. As might be expected, the maximum pressure increases with increasing void radius and colloid volume fraction (figure 6). From a practical point of view it is interesting to know for how long the pressure inside the void exceeds the threshold pressure for cleavage of the matrix (figure 7). The longer this time interval, τ, the larger the distance that the crack will travel. Figure 8 depicts the dependence of τ on the void radius and colloid volume fraction

The results of the numerical calculations show that the temperature increases very rapidly, and then decreases relatively slowly as $t^{-1/2}$. Therefore, we may assume that the back reaction occurs instantaneously, and afterward the voids cool down by heat conduction into the matrix. It is useful to approximate the time dependence of the temperature decrease on the basis of the simple model shown in figure 9. The heat released during the reaction is distributed between
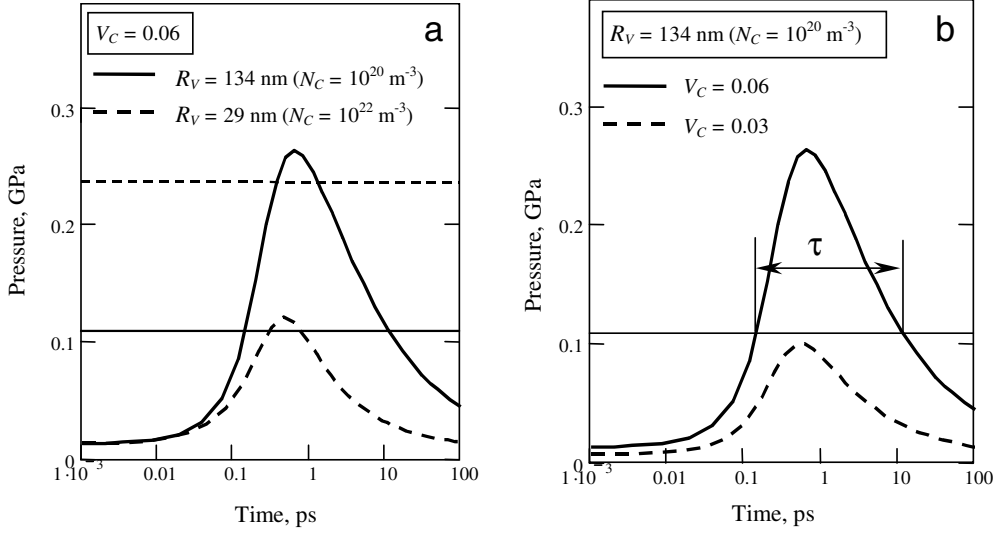
Figure 5. The pressure created by the hot gas inside the void. The horizontal lines refer to the threshold pressure given by (14). τ is the time interval during which a crack may start propagating from the overpressurized void.
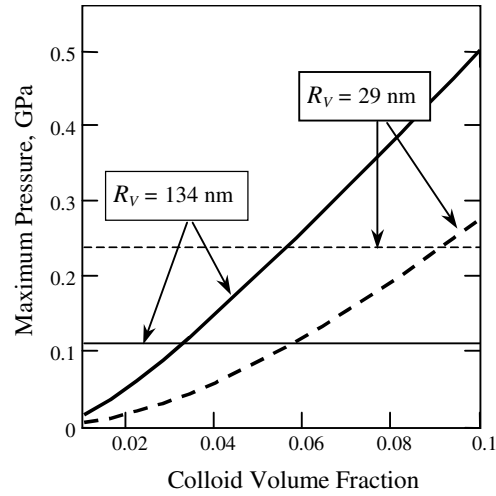

Figure 6. Maximum pressure inside the void versus the Na colloid fraction. The horizontal lines correspond to the threshold cleavage pressure given by (14).

NaCl gas in the void and the spherical shell of thickness ΔR in the crystalline NaCl matrix, assuming that both parts of the system have the same temperature, which we want to calculate. $\Delta R(t)$ is the distance reached by the temperature front at time t:

$$\frac{4\pi}{3\omega} R_V^3 V_C C_2 T_{max} = \left(\frac{4\pi}{3\omega} R_V^3 V_C C_2 + 4\pi R_V^2 \, \Delta R(t) \, C_m d_m \right) T_{\text{Cooling}}. \qquad (16)$$

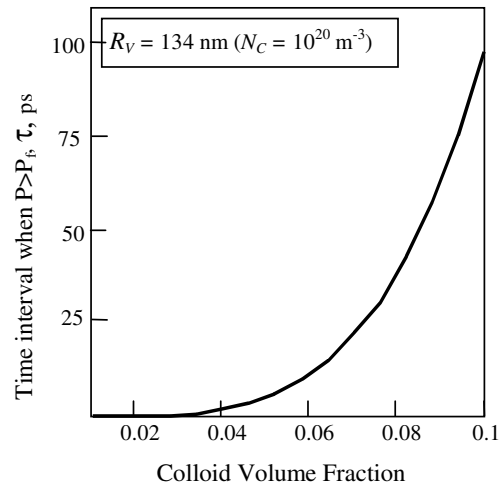Here ΔR was assumed to be smaller than R_V. This is reasonable because of a small heat

Figure 7. Time interval τ (in picoseconds) during which a crack may start propagating from a void versus the colloid volume fraction.
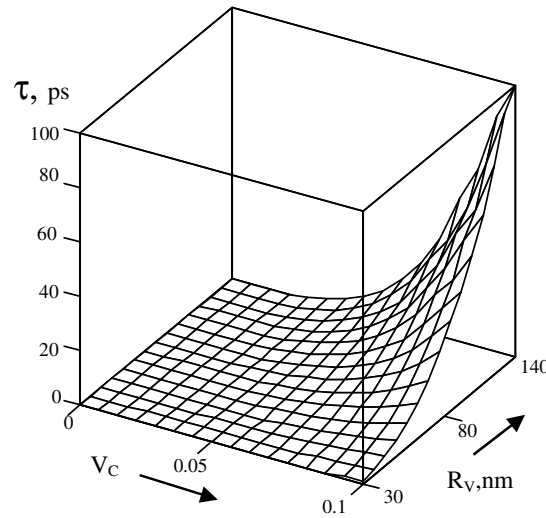

Figure 8. Time interval (in picoseconds) during which a crack may start propagating from a void, τ, versus colloid volume fraction, V_C, and the void explosion radius, R_V.

capacity of the gas inside the void as compared to that of the matrix:

$$\left. \frac{C_m d_m \omega}{C_2 V_C} \right|_{V_C=0.06} = 35. \tag{17}$$

Setting $\Delta R = \sqrt{2at}$ yields

$$T_{\text{Cooling}} = T_{max} \left(1 + \frac{3}{R_V} \frac{C_m d_m \omega}{C_2 V_C} \sqrt{2at} \right)^{-1} \tag{18}$$

which is in a good agreement with numerical results (figure 10). Using (18) we can calculate
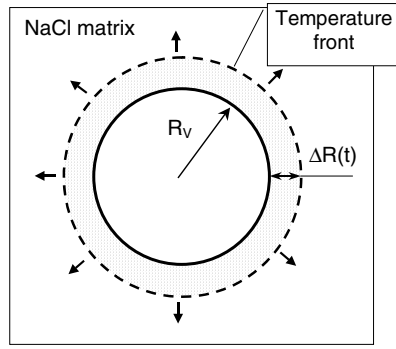
Figure 9. A model of the void cooling due to dissipation of heat in the matrix layer of thickness $\Delta R(t)$, which expands with time.
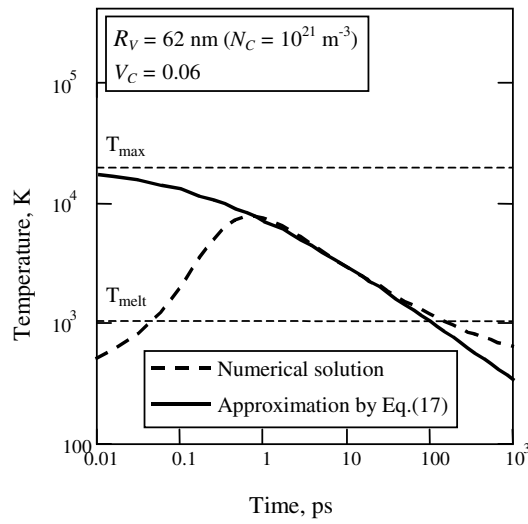

Figure 10. Comparison of numerical results on the void cooling with the analytical approximation (18) shown in figure 9.

the pressure inside the void during the cooling stage with the following relation:

$$P_{\text{Cooling}} = \frac{V_C}{\omega} k_B T_{\text{Cooling}}. \tag{19}$$

From (14) and (19) we obtain an analytical expression for the time interval τ, which agrees well with the numerical results:

$$\tau = \frac{R_V^2}{18a} \left(\frac{C_2 V_C}{C_m d_m \omega} \right)^2 \left[2k_B T_{max} \frac{V_C}{\omega} \sqrt{R_V} \sqrt{\frac{2\pi(1-\nu^2)}{G_C E}} - 1 \right]^2. \tag{20}$$

The first term of this expression is proportional to

$$R_V^3 V_C^4 \propto N_C^{-1} V_C^4$$

which shows that the maximum size of the voids (determined by the colloid number density) is as important for the material stability as the colloid volume fraction.

5. Discussion

As we have shown above, the ultimate pressure increase within the voids induced by the back reaction increases almost linearly with increasing colloid volume fraction and can exceed a threshold pressure P_f required for the crack propagation from the void along one of the matrix cleavage planes (100) in the absence of an external load [18].

Another important parameter of the back reaction is a time interval, τ, during which the pressure exceeds the threshold value. If this time interval is long enough, the crack may sweep adjacent chlorine and sodium precipitates, which fill the crack. This process would add new 'fuel' for the ongoing back reaction. The final crack length in such cases is determined by the rates of two competing processes, namely the production and dissipation of the heat [19]. The heat production is determined by the rate of expansion of the crack volume, which is determined by the length and thickness (due to cleavage and dislocation emission, respectively) of the cracks and the rate at which new fuel is collected by the cracks. Ultimately, this process results in 'burning' of the new fuel, which increases the pressure by a factor proportional to
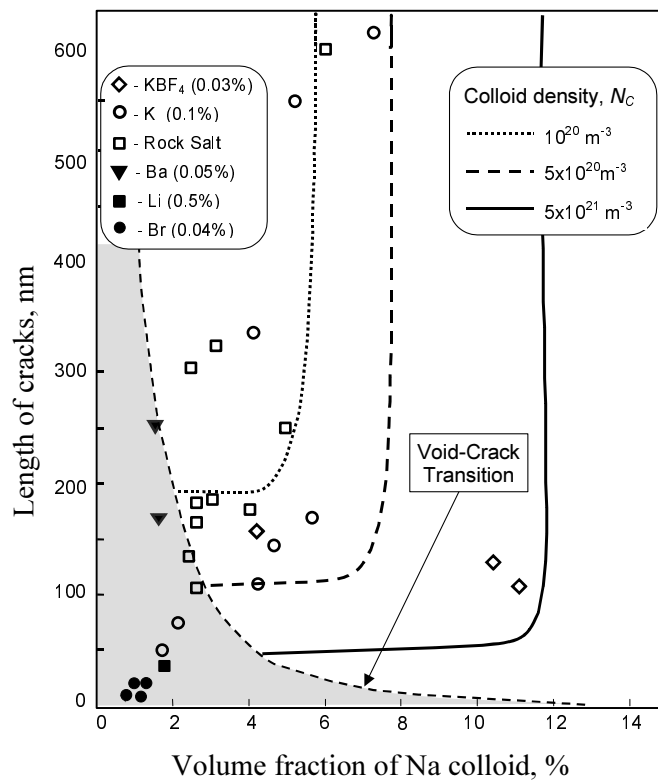

Figure 11. A diagram showing the dependence of the maximum void size and the subsequent crack length on the colloid volume fraction, calculated for different colloid number densities, N_C, assuming that the crack propagation rate equals the speed of sound in NaCl. The explosive fracture of the material starts at the point where the crack length derivative with respect to the colloid volume fraction becomes infinite. Above these points, no stable crack exists, which implies that the positive feedback due to consumption of new 'fuel' becomes stronger than the negative feedback due to the heat dissipation. Experimental points correspond to the maximum diameter of voids/cracks observed in materials with different dopants (concentrations are given in mol%), for which the measured values of N_C increase in the following sequence [11]: Br, Li, Ba, rock salt, K, KBrF$_4$.

the surface covered by the propagating crack, its thickness and the colloid volume fraction. The heat dissipation is determined mainly by the propagation rate of the temperature front (figure 9), which is heated at the expense of the energy released in the back reaction, which reduces the gas pressure. The crack propagation stops as soon as the gas pressure falls below the threshold value. Accordingly, the final crack length is determined by the volume fraction and the number density of colloids, the crack propagation rate and material parameters, such as the thermal conductivity of NaCl and the total work of fracture [11, 19]. At sufficiently large colloid volume fraction, the heat production starts to dominate over its dissipation, resulting in unrestricted crack propagation. The result is shown in figure 11 in the form of the crack length dependence on the colloid volume fraction at different colloid number densities. Different dopants have been shown to result in colloid number densities, N_C, increasing in the following sequence [11]: Br, Li, Ba, Dutch rock salt, K, KBrF$_4$. In this way the dopants can determine the void explosion radius, which has a drastic effect on the ultimate mechanical stability of the material. In NaCl:Br (the minimum N_C) the void explosion radius is large as compared to the observed ones, and we have found that these samples remain mechanically stable up to the highest dose reached so far. In NaCl:KBF$_4$ (the maximum N_C), the void explosion radius is comparable with the radii of observed voids, but a higher colloid volume fraction is required to initiate the void–crack transition than that achieved in these samples. Accordingly, even at the highest damage levels it was difficult to initiate explosive decomposition during irradiation of KBF$_4$-doped samples. The materials doped with Ba or K and natural rock salt show the transitional behaviour, which is characterized by an early start and rapid progress of the void–crack transition, resulting in a subsequent explosive fracture of the material due to unrestricted propagation of cracks.

Acknowledgments

References

[1] Lidiard A B 1978 *Comment. Solid State Phys.* **8** 73
[2] Lidiard A B 1979 *Phil. Mag.* **39** 647
[3] den Hartog H W, Groote J C and Weerkamp J R W 1996 *Radiat. Eff. Defects Solids* **139** 1
[4] Vainshtein D I, Altena C and den Hartog H W 1997 *Mater. Sci. Forum.* **239–241** 607
[5] den Hartog H W and Vainshtein D I 1997 *Mater. Sci. Forum.* **239–241** 611
[6] Vainshtein D I and den Hartog H W 2000 *Radiat. Eff. Defects Solids* **152** 23
[7] Dubinko V I, Turkin A A, Vainshtein D I and den Hartog H W 1999 *J. Appl. Phys.* **86** 5957
[8] Dubinko V I, Turkin A A, Vainshtein D I and den Hartog H W 2000 *J. Nucl. Mater.* **227** 184
[9] Dubinko V I, Turkin A A, Vainshtein D I and den Hartog H W 2001 *6th Symp. on Fabrication and Properties of Ceramics for Fusion Energy and Other High Radiation Environments (St Louis); J. Nucl. Mater.* at press
[10] Vainshtein D I, Dubinko V I, Turkin A A and den Hartog H W 2000 *Nucl. Instrum. Methods Phys. Res.* B **166+167** 550
[11] den Hartog H W, Vainshtein D I, Dubinko V I, Turkin A A, Gann V V and Jacobs J 1999 Radiation damage in NaCl: retrievability, smart backfill materials, monitoring *CORA Research Project for the Dutch Ministry of Economic Affairs Final Report* December 1999
[12] Levine R D and Bernstein R B 1987 *Molecular Reaction Dynamics* (Oxford: Oxford University Press)
[13] Kondrat'ev V N 1964 *Chemical Kinetics of Gas Reactions* (Oxford: Pergamon)
[14] Smoluchowski M V 1917 *Z. Phys. Chem.* **92** 129
[15] Kuzmichev V E 1989 *Physics Laws and Formulae. Handbook* (Kiev: Naukova Dumka) (in Russian)

[16] Budak B M, Samarskii A A and Tikhonov A N 1964 *A Collection of Problems on Mathematical Physics* (Oxford: Pergamon)

[17] Press W H, Teukolsky S A, Vetterling W T and Flannery B P 1992 *Numerical Recipes in Fortran 77: the Art of Scientific Computing* 2nd edn (Cambridge: Cambridge University Press)

[18] Voskoboinikov R E 1999 *J. Nucl. Mater.* **270** 309

[19] Dubinko V I, Turkin A A, Vainshtein D I and den Hartog H W 2001 *ICDIM-2000 (Johannesburg, South Africa); Radiat. Eff. Defects Solids* at press